

Rotational structures near $40\hbar$ in ^{123}La

H. I. Park, D. J. Hartley,* L. L. Riedinger, W. Reviol,† O. Zeidan,‡ and Jing-Ye Zhang
Department of Physics and Astronomy, University of Tennessee, Knoxville, Tennessee 37996, USA

A. Galindo-Uribarri
Physics Division, Oak Ridge National Laboratory, Oak Ridge, Tennessee 37831, USA

R. V. F. Janssens, M. P. Carpenter, and D. Seweryniak
Physics Division, Argonne National Laboratory, Argonne, Illinois 60439, USA

D. G. Sarantites and M. Devlin§
Chemistry Department, Washington University, St. Louis, Missouri 63130, USA

B. G. Dong|| and I. Ragnarsson
Department of Mathematical Physics, Lund Institute of Technology, Box 118, S-22100 Lund, Sweden
 (Received 21 July 2003; published 31 October 2003)

The neutron-deficient nucleus ^{123}La was studied via the $^{92}\text{Mo}(^{40}\text{Ca}, 2ap)$ reaction at a beam energy of 184 MeV. Previously known bands were extended to a much higher spin, and in two cases the structures are now observed near $40\hbar$. In addition, three new sequences were identified and linked into previously known bands. The lowest $(\pi, \alpha) = (+, -\frac{1}{2})$ structure displays characteristics similar to those of analogous bands in $^{127,129}\text{La}$, which have been proposed as examples of smooth band termination. Cranked Nilsson-Strutinsky calculations were compared with the experimental data in ^{123}La to determine whether this band is approaching a terminating state as well.

DOI: 10.1103/PhysRevC.68.044323

PACS number(s): 21.10.Re, 23.20.Lv, 27.60.+j

I. INTRODUCTION

The lanthanum nuclei, having only seven protons outside the $Z=50$ shell gap, are located in a transitional region between vibrational and well-deformed nuclei. In isotopes near $N=75$, this has led to prolate-oblate shape coexistence in ^{131}La [1], as well as to the possibility of triaxial deformation based on the claims of chiral-twin bands in $^{132,134}\text{La}$ [2,3]. As the La nuclei become more proton rich and approach mid-shell at $N=64$, they become more resilient to shapedriving effects at lower spins. However, recent calculations suggest that shape coexistence may occur in La nuclei at very high spins [$I=(40-50)\hbar$] in the form of smooth band termination [4]. Indeed, experimental evidence for this phenomenon was observed in $^{127,129}\text{La}$ [5,6]. Therefore, it is of interest to investigate whether this phenomenon can be observed over a broad range of La nuclei. A previous study of ^{125}La [7] did not show any indication of band termination at the highest

observed states ($I \approx 35\hbar$). However, the present prediction of terminating states below $50\hbar$ for ^{123}La was a motivating factor to study this nucleus.

In an experiment designed to study high-spin states in severely neutron-deficient rare-earth nuclei, the nucleus ^{123}La was produced in a relatively weak reaction channel. However, the sensitivity of the Gammasphere γ -ray array [8] and the selectivity of the Microball charged-particle array [9] allowed for the extension of previously known structures [10] to angular momentum values near $40\hbar$. As mentioned above, this is near the region of predicted band termination for La nuclei. Characteristics of the lowest $(\pi, \alpha) = (+, -\frac{1}{2})$ band in ^{123}La are apparently consistent with smooth band termination. Therefore, an investigation into possible termination has been performed by comparing the experimental data with cranked Nilsson-Strutinsky calculations. In addition, three new sequences have been associated with ^{123}La , and configurations have been proposed for each.

II. EXPERIMENTAL DETAILS

The reaction $^{40}\text{Ca} + ^{92}\text{Mo}$ was used to produce these light rare-earth nuclei with $Z=57-60$. A beam energy of 184 MeV was selected and the target consisted of a 0.625 mg/cm^2 self-supporting foil of ^{92}Mo . The experiment was performed at Argonne National Laboratory and utilized Gammasphere [8] in combination with the Washington University Microball [9]. Gammasphere consisted of 99 Ge detectors for this experiment. Although ^{123}La was populated in a relatively weak reaction channel ($\sim 1.3\%$ of the $\sim 580 \times 10^6$ five-fold or

*Present address: Department of Physics, United States Naval Academy, Annapolis, Maryland 21402.

†Present address: Chemistry Department, Washington University, St. Louis Missouri 63130.

‡Present address: Department of Radiation Oncology, University of Florida, Gainesville, Florida 32610.

§Present address: Los Alamos National Laboratory, Los Alamos, New Mexico 87545.

||Present address: Department of Nuclear Physics, China Institute of Atomic Energy, P.O. Box 275 (18), Beijing 102413, China.

higher events recorded), the selectivity of the Microball allowed for an extremely clean separation of γ rays in coincidence with the $2\alpha p$ channel leading to ^{123}La . These transitions were corrected for Doppler shifts and sorted into an $E_\gamma \times E_\gamma \times E_\gamma$ cube that was inspected with the RADWARE [11] analysis package.

The relative spin assignments were determined through a directional angular correlation of oriented states (DCO) analysis. To obtain this information with sufficient statistics, an angle-dependent $E_\gamma \times E_\gamma$ matrix was created, where the energies of γ rays observed in detectors located at 31.7° , 37.4° , 50.1° , 129.9° , 142.6° , and 148.3° [symmetric forward and backward (FB) angles] were projected along one axis and coincident γ rays observed in detectors located at 79.2° , 80.7° , 90.0° , 99.3° , and 100.8° were projected along the other. DCO ratios were determined by the following expression:

$$R_{DCO} = \frac{I_{\gamma_1}(\text{at FB, in coincidence with } \gamma_2 \text{ at } \sim 90^\circ)}{I_{\gamma_1}(\text{at } \sim 90^\circ, \text{ in coincidence with } \gamma_2 \text{ at FB})},$$

where I_{γ_1} is the intensity of the γ ray of interest and γ_2 is a stretched $E2(\Delta I=2)$ transition. With the detectors at the given angles, expected R_{DCO} values are approximately 0.5 for pure dipole transitions ($M1$ and $E1$) and 1.0 for quadrupole transitions ($E2$). The measured DCO ratios are summarized in Table I along with the energy, spin, and parity of the states, as well as the relative intensity of the depopulating γ rays. Where the statistics were too low to perform DCO analysis, multipolarities were assigned assuming that rotational band characteristics persist.

III. LEVEL SCHEME

In an earlier work on ^{123}La [10], three rotational bands were identified, but no linking transitions were observed between the bands. The level scheme for ^{123}La deduced from the present work is given in Fig. 1. The previously known structures were extended to much higher spins, and are labeled as bands 1, 3, and 6 in Fig. 1. In addition, three new structures, labeled as bands 2, 4, and 5, were also identified. Linking transitions were established for the first time between bands 1–5 and as a result, the relative excitation energies of these sequences are now firmly established. The ordering of transitions in the level scheme was based on the observed coincidence relationships and the measured relative intensities. Spin and parity assignments for bands 1, 3, and 6 were suggested by Wyss *et al.* [10] on the basis of systematics, observed band crossing behavior, and the single-particle orbitals expected near the Fermi surface. We are in agreement with these assignments, however, these, along with all new assignments, must be considered as tentative since the spin/parity of the ground state has not been established through a direct measurement.

Prior to our work, band 1 was reported up to $I^\pi = \frac{55}{2}^+$ [10]; it is now extended to $I^\pi = (\frac{79}{2})^+$. A spectrum of band 1 is shown in Fig. 2(a), which is a result of summing all possible combinations of double coincidence gates above the $\frac{35}{2}$ state. There are two transitions decaying from the $\frac{7}{2}$ state with en-

TABLE I. γ ray energies and intensities in ^{123}La .

$I_i^{\pi a}$	$E_{\text{level}}(\text{keV})$	$E_\gamma(\text{keV})^b$	I_γ^c	DCO
Band 1				
$\frac{7}{2}^+$	224.4	189.0	19(3)	0.91(2)
		224.4	~ 7	0.69(4)
$\frac{11}{2}^+$	549.3	324.9	28(2)	0.93(2)
		509.9	5.0(5)	
$\frac{15}{2}^+$	987.5	438.2	35(1)	0.98(2)
		717.0	3.9(2)	0.9(1)
$\frac{19}{2}^+$	1487.5	500.0	37(2)	1.02(2)
		814	< 2	
$\frac{23}{2}^+$	1979.5	492.0	36(1)	0.96(2)
$\frac{27}{2}^+$	2519.1	539.6	32(1)	1.08(2)
$\frac{31}{2}^+$	3152.7	633.6	30.7(9)	1.11(3)
$\frac{35}{2}^+$	3882.8	730.1	27.0(7)	0.95(2)
$\frac{39}{2}^+$	4703.6	820.8	21.6(5)	1.05(5)
$\frac{43}{2}^+$	5607.6	904.0	15.9(4)	1.09(4)
$\frac{47}{2}^+$	6589.8	982.2	11.3(3)	1.17(5)
$\frac{51}{2}^+$	7650.2	1060.4	7.7(2)	1.10(7)
$\frac{55}{2}^+$	8791.9	1141.7	5.4(8)	1.02(8)
$\frac{59}{2}^+$	10020.2	1228.3	2.9(2)	1.02(12)
$\frac{63}{2}^+$	11338.3	1318.1	< 2	
$\frac{67}{2}^+$	12753.1	1414.8	< 2	
$\frac{71}{2}^+$	14272.3	1519.2	< 2	
$\frac{75}{2}^+$	15896.5	1624.2	< 2	
$\frac{79}{2}^+$	(17652)	(1755)	< 2	
Band 2				
$\frac{21}{2}^+$	1797.9	1123.5	< 2	
$\frac{25}{2}^+$	2325.3	527.4	< 2	
		1101.9	4.0(5)	0.46(7)
$\frac{29}{2}^+$	2905.9	580.6	6.7(4)	
		1011.5	7.7(6)	0.56(4)
$\frac{33}{2}^+$	3574.0	668.1	13.2(5)	
		911.6	3.9(3)	0.64(4)
$\frac{37}{2}^+$	4336.6	762.6	15.2(6)	
$\frac{41}{2}^+$	5189.5	852.9	14.0(5)	
$\frac{45}{2}^+$	6131.3	941.8	9.7(5)	
$\frac{49}{2}^+$	7168.2	1036.9	8.8(4)	
$\frac{53}{2}^+$	8306.5	1138.3	4.1(2)	
$\frac{57}{2}^+$	9550.3	1243.8	2.5(2)	
$\frac{61}{2}^+$	10892.5	1342.2	< 2	
$\frac{65}{2}^+$	12327.1	1434.6	< 2	
$\frac{69}{2}^+$	(13852)	(1525)	< 2	
Band 3				
$\frac{11}{2}^-$	39.8			
$\frac{15}{2}^-$	270.5	230.7	~ 120	0.91(1)
$\frac{19}{2}^-$	673.8	403.3	$\equiv 100$	0.94(2)
$\frac{23}{2}^-$	1223.8	550.0	83(4)	1.00(1)
$\frac{27}{2}^-$	1894.4	670.6	71(3)	1.00(2)
$\frac{31}{2}^-$	2662.4	768.0	50(2)	1.02(3)
$\frac{35}{2}^-$	3512.1	849.7	31(2)	1.00(4)
$\frac{39}{2}^-$	4437.5	925.4	24(1)	0.97(4)
$\frac{43}{2}^-$	5437.9	1000.4	16.3(6)	1.00(5)

TABLE I. (Continued.)

$I_i^{\pi a}$	$E_{level}(\text{keV})$	$E_\gamma(\text{keV})^b$	I_γ^c	DCO
$\frac{47}{2}-$	6510.9	1073.0	13.3(6)	0.94(7)
$\frac{51}{2}-$	7652.8	1141.9	9.6(4)	1.37(9)
$\frac{55}{2}-$	8863.5	1210.7	4.8(2)	
$\frac{59}{2}-$	10142.3	1278.8	4.5(2)	
$\frac{63}{2}-$	11490.3	1348.0	<2	
$\frac{67}{2}-$	12909.7	1419.4	<2	
$\frac{71}{2}-$	14408.4	1498.7	<2	
$\frac{75}{2}-$	15993.1	1584.7	<2	
$\frac{79}{2}-$	(17663)	(1670)	<2	
		Band 4		
$\frac{15}{2}-$	957.1	687.0	2.0(4)	
		917.5	<2	
$\frac{19}{2}-$	1351.8	394.7	2.8(3)	
		678.0	3.4(3)	
		1081.4	5.0(8)	
$\frac{23}{2}-$	1856.1	504.3	9.2(3)	
		1182.3	3.4(4)	
$\frac{27}{2}-$	2466.4	610.3	9.5(4)	
		1242	<2	
$\frac{31}{2}-$	3173.2	706.8	6.8(3)	
$\frac{35}{2}-$	3968.2	795.0	4.8(5)	
$\frac{39}{2}-$	4851.9	883.7	4.3(3)	
$\frac{43}{2}-$	5830.1	978.2	3.4(3)	
$\frac{47}{2}-$	6905.4	1075.3	2.5(3)	
$\frac{51}{2}-$	8068.1	1162.7	2.0(3)	
$\frac{55}{2}-$	(9289)	(1221)	<2	
		Band 5		
$\frac{21}{2}-$	1735.3	(1062)	<2	
$\frac{25}{2}-$	2304.1	568.8	<2	
		1080.3	3.7(6)	
$\frac{29}{2}-$	2968.4	664.3	3.3(4)	
		1072	<2	
$\frac{33}{2}-$	3727.4	759.0	5.0(4)	
$\frac{37}{2}-$	4571.3	843.9	4.7(3)	
$\frac{41}{2}-$	5498.3	927.0	4.3(3)	
$\frac{45}{2}-$	6503.6	1005.3	2.8(3)	
$\frac{49}{2}-$	7579.7	1076.1	<2	
$\frac{53}{2}-$	8701	1121	<2	
		Band 6		
$\frac{11}{2}+$	X+209.5	209.5	~ 45	0.55(6)
$\frac{15}{2}+$	X+716.1	506.6	10.2(5)	
		267.1	23(1)	0.55(6)
$\frac{19}{2}+$	X+1322.4	606.3	13.1(6)	
$\frac{g}{2}+$		314.4	15.4(6)	0.52(5)
$\frac{23}{2}+$	X+2005.0	682.6	13.0(6)	
		349.7	7.4(3)	0.58(6)
$\frac{27}{2}+$	X+2724.7	719.7	11.9(6)	
		359.5	7.0(3)	0.58(6)
$\frac{31}{2}+$	X+3417.0	692.3	11.3(6)	
		342.9	4.5(2)	0.55(6)
$\frac{35}{2}+$	X+4132.1	715.1	7.8(4)	

TABLE I. (Continued.)

$I_i^{\pi a}$	$E_{level}(\text{keV})$	$E_\gamma(\text{keV})^b$	I_γ^c	DCO
		369.2	3.3(2)	0.54(7)
$\frac{39}{2}+$	X+4937.4	805.3	7.8(4)	
		417.9	2.2(2)	0.53(8)
$\frac{43}{2}+$	X+5840.8	903.4	5.3(3)	
		467.0	1.8(1)	
$\frac{47}{2}+$	X+6842.1	1001.3	5.0(3)	
$\frac{51}{2}+$	X+7938.0	1095.9	4.8(3)	
$\frac{55}{2}+$	X+9132.3	1194.3	2.9(2)	
$\frac{59}{2}+$	X+10425.2	1292.9	<2	
$\frac{63}{2}+$	X+11810.9	1385.7	<2	
		Band 6		
$\frac{13}{2}+$	X+449.2	449.2	6.0(3)	
		239.5	31(1)	0.58(6)
$\frac{17}{2}+$	X+1008.5	559.3	13.4(6)	
		292.1	18.5(8)	0.54(6)
$\frac{21}{2}+$	X+1656.3	647.8	13.4(6)	
		333.6	11.5(5)	0.59(6)
$\frac{25}{2}+$	X+2365.5	709.2	13.4(7)	
		360.1	7.2(4)	0.57(6)
$\frac{29}{2}+$	X+3075.1	709.6	12.9(7)	
		349.4	5.7(4)	0.58(6)
$\frac{33}{2}+$	X+3763.2	688.1	9.8(5)	
		346.1	3.7(2)	
$\frac{37}{2}+$	X+4519.5	756.3	9.4(4)	
		387.1	2.9(2)	0.72(17)
$\frac{41}{2}+$	X+5373.8	854.3	7.2(4)	
		436.4	1.8(2)	0.55(7)
$\frac{45}{2}+$	X+6326.8	953.0	5.1(3)	
		485.8	1.7(1)	
$\frac{49}{2}+$	X+7375.8	1049.0	5.1(3)	
$\frac{53}{2}+$	X+8521.9	1146.1	5.1(3)	
$\frac{57}{2}+$	X+9765.6	1243.7	4.0(2)	
$\frac{61}{2}+$	X+11107.0	1341.4	<2	
$\frac{65}{2}+$	X+12541.9	1434.9	<2	

^aSpin and parity of the depopulated state.^bUncertainties in E_γ are 0.2 keV for most transitions, except for relatively weak transitions where 0.5 keV uncertainties are appropriate.^cRelative intensity of the transition where $I_\gamma(403.3) \equiv 100$.

ergies of 189.0 keV and 224.4 keV (see Fig. 1). A DCO ratio of 0.91(2) suggests that the former γ ray is an $E2$ transition while the 224.4 keV γ ray is likely a $\Delta I=1$ transition due to its measured ratio $R_{DCO}=0.69(4)$. Thus, the 189.0-keV transition is placed as an inband transition in Fig. 1 and the 224.4-keV γ ray is shown as a decay to the lowest observed state in ^{123}La . It is possible that this is the ground state, however, a recent β decay experiment could not determine the ground-state spin or parity [12]. Although band 1 is ~ 700 keV above the yrast sequence (band 3) at low spin ($I \leq \frac{15}{2}$), it becomes yrast at and above $I = \frac{51}{2}$. Linking transitions were observed between bands 1 and 3 (see Fig. 1) and a DCO ratio of 0.9(1) was determined for the 717.0-keV γ

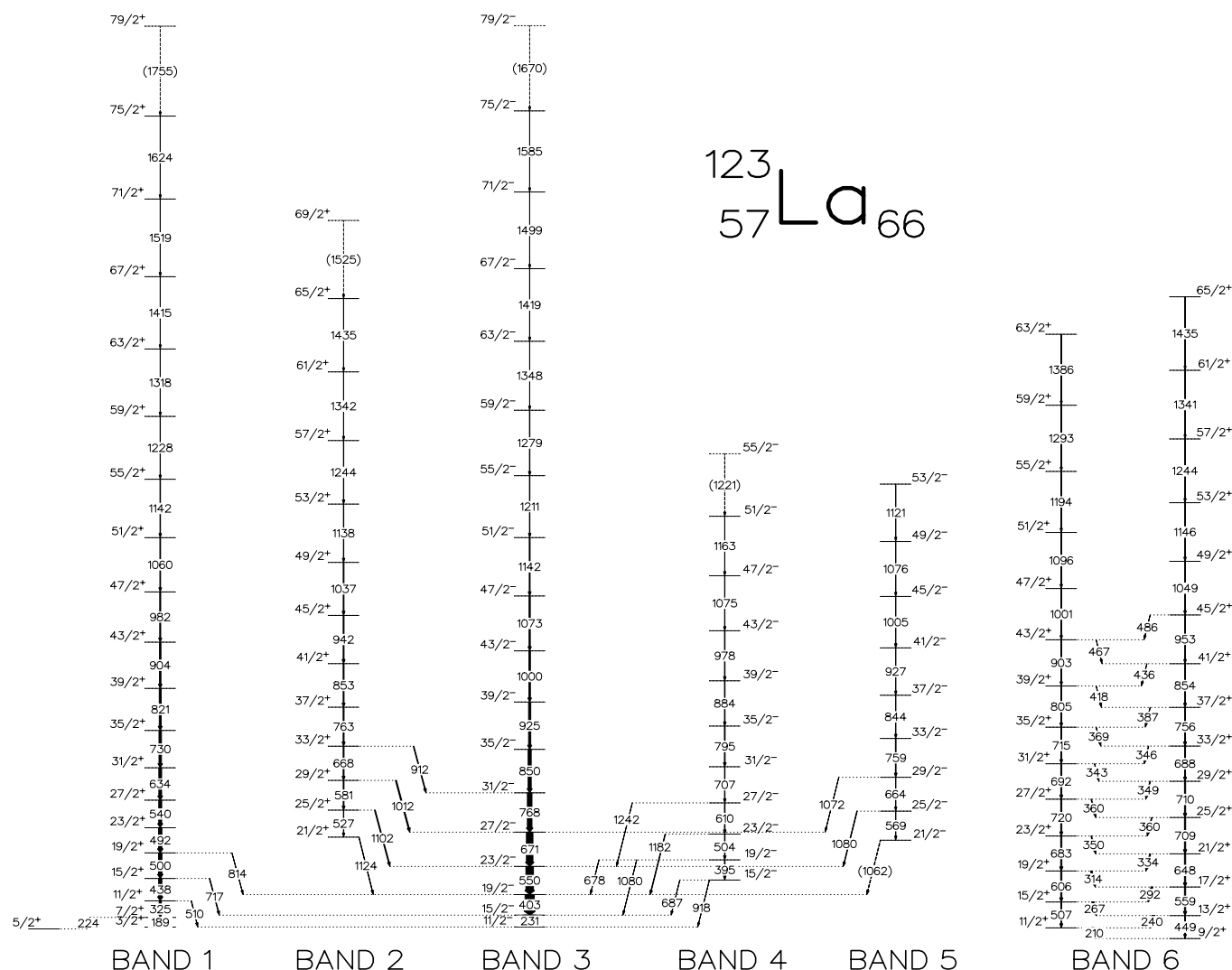


FIG. 1. The level scheme proposed for ^{123}La . The width of the arrows is proportional to the transition intensity. Tentative transitions are denoted by dashed lines. Spin and parity assignments are considered tentative as explained in the text.

ray. From systematics of similar bands [14], the linking γ rays are likely $I \rightarrow I$ transitions (consistent with the measured DCO ratio), thus resulting in a bandhead spin of $\frac{3}{2}$. This is in good agreement with the proposed configuration of band 1, as discussed below, and the assignment in Ref. [10].

As previously stated, band 2 was observed for the first time and a representative spectrum is shown in Fig. 2(b). The four lowest states of this band strongly feed band 3 through high-energy transitions. The DCO analysis indicates that the 911.6-keV, 1011.5-keV, and 1101.9-keV linking transitions are nearly of pure dipole character (see Table I), which suggests that they most likely correspond to $E1$ transitions. Thus, $I^\pi = \frac{21}{2}^+$ has been assigned to the 1797.9-keV level in band 2 as odd parity is associated with band 3 (see below). It is interesting to note that while bands 1 and 2 both have even parity, no linking transition between the sequences was observed. Band 2 was observed up to a relatively high angular momentum state of $(\frac{69}{2})$.

Band 3, as displayed in the level scheme of Fig. 1, is the most intensely populated structure at lower spins in ^{123}La . Wyss *et al.* [10] proposed the $\frac{11}{2}^-$ assignment for the initial

state based on the systematics of heavier La isotopes and its suggested configuration. In a β -decay study [12], states of spins $\frac{7}{2}$, $\frac{9}{2}$, and $\frac{11}{2}$ in ^{123}Ba were directly fed by ^{123}La . This indicates the presence of a high-spin ground state or of a β -decaying isomer in ^{123}La . From the present work, it is clear that the $\frac{11}{2}^-$ level is not the ground state as it lies 4 keV above the bandhead of band 1 and 40 keV above the lowest state observed. However, as the transition decaying from the $\frac{11}{2}^-$ bandhead of band 3 to the possible ground state is of low energy (~ 40 keV) and high multipolarity (perhaps $E3$), the lifetime of the $\frac{11}{2}^-$ state is likely quite long [on the order of a second according to Fig. 5.2 in Ref. [13]] such that β decay from this level is certainly possible. The present data allowed for the extension of this band from $\frac{59}{2}^-$ to $\frac{79}{2}^-$ and a representative spectrum is given in Fig. 3(a).

The lowest state in band 4 was observed at an energy of 957.1 keV. It decays into both the $\frac{11}{2}$ and $\frac{15}{2}$ states of band 3. These linking transitions, plus those coming from higher-spin states, can be observed in the sample spectrum provided in Fig. 3(b). This decay pattern limits the choices of spin for

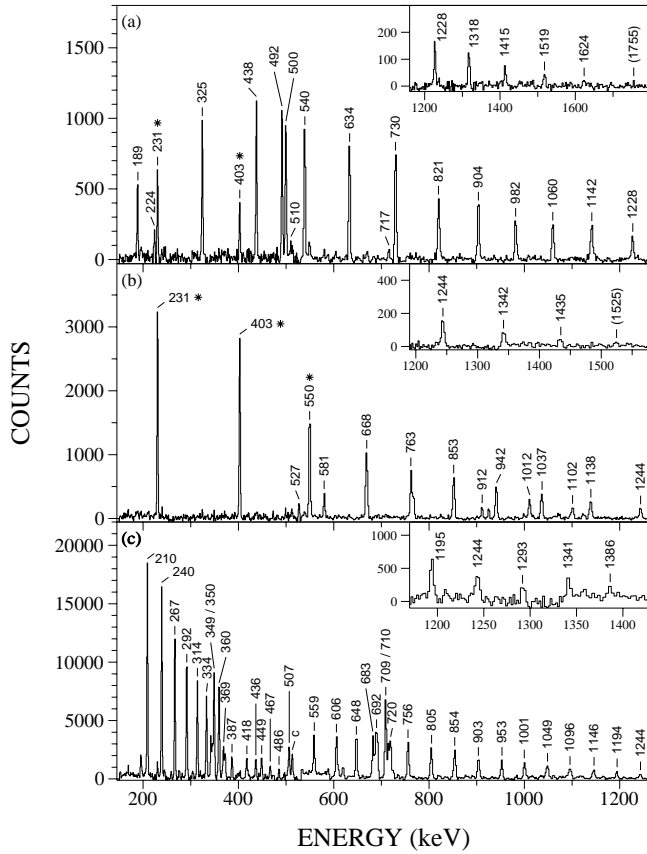


FIG. 2. (a) Spectrum of band 1 produced by summing all possible combinations of double coincidence gates above the $\frac{35}{2}$ state. (b) Spectrum for band 2 resulting from a sum of spectra over all possible double-gate combinations of the in-band transitions. (c) The spectrum for band 6 obtained by summing all clean double-gated spectra of in-band transitions. The high-energy transitions of all bands are displayed in insets, and peaks denoted by * are associated with band 3.

the lowest state to either $\frac{13}{2}$ or $\frac{15}{2}$ as only $E1$, $M1$, and $E2$ transitions are normally observed in prompt spectroscopy. Unfortunately, the linking transitions from this structure to band 3 were too weak to obtain meaningful DCO ratios. A spin of $I=\frac{15}{2}$ is favored for the 957.1-keV level based upon energy and population intensity considerations; however, a $\frac{13}{2}$ assignment cannot be completely ruled out. In addition, the decay and in-band characteristics of this sequence are similar to a structure in ^{125}La (labeled as band 6 in Ref. [7]) whose lowest state was determined to have $\frac{15}{2}$ quantum numbers. Thus, odd parity is also tentatively assigned to band 4 in ^{123}La .

The weakest structure observed in ^{123}La is denoted as band 5 in Fig. 1 and a spectrum is presented in Fig. 3(c). Once again, relative spin assignments could not be proposed from a DCO analysis due to insufficient statistics. However, since band 5 was seen as high in energy as band 4, it is likely that these bands are relatively close in energy at their highest observed spins. Therefore, a spin of $I=\frac{21}{2}$ has been tentatively assigned for the lowest state, which suggests that the linking transitions are likely dipoles. A tentative odd-parity assign-

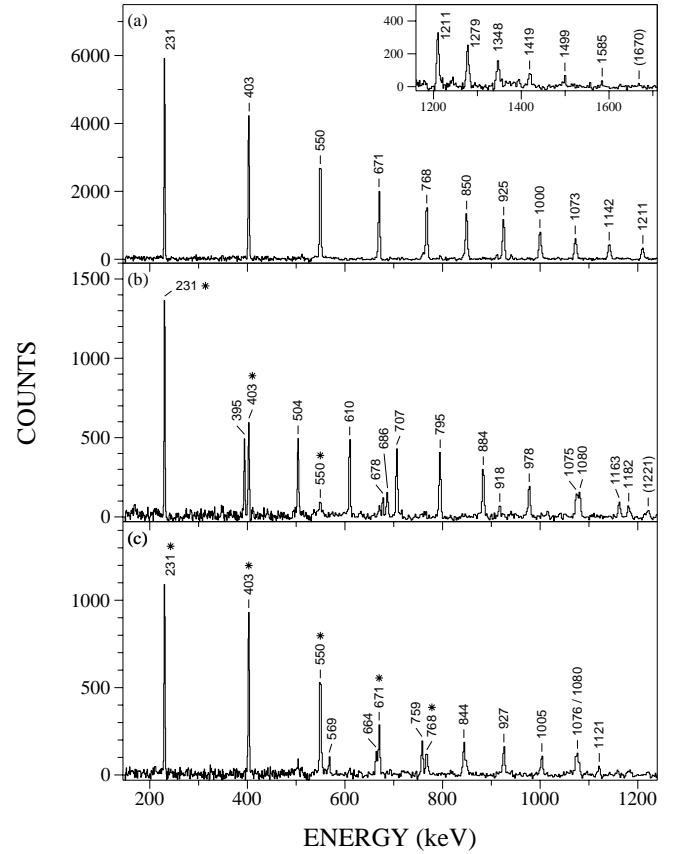


FIG. 3. (a) Spectrum for band 3 produced by summing all possible combinations of double coincidence gates above the $\frac{23}{2}$ state. (b) Spectrum for band 4 created by summing spectra for all possible combinations of double-gated spectra placed on in-band transitions. (c) Spectrum for band 5, which was the result of the same procedure as described for band 4.

ment has been given, based upon the proposed configuration discussed below.

The strongly coupled sequence labeled as band 6 in Fig. 1 was assigned a $\frac{9}{2}^+$ bandhead spin/parity based on the proposed configuration in Ref. [10]. This structure was extended to $\frac{65}{2}^+$ with the present data and a spectrum for both signatures is shown in Fig. 2(c). No linking transitions were observed between this structure and the other bands in ^{123}La . Indeed, inspection of Fig. 2(c) reveals that there are no coincidence relations with any of the other sequences presented above. Thus, it is likely that band 6 also has an isomeric bandhead with a lifetime greater than that of the prompt time gate (~ 80 ns) used for this analysis. It should be noted that a similar structure in ^{125}La appears to be based on an isomeric state as well [7].

IV. DISCUSSION

A. Cranked shell model calculations

In order to facilitate a discussion of the configurations associated with the structures in ^{123}La , the aligned angular momenta of bands 1–6 are plotted as a function of rotational frequency in Fig. 4. The ground-state band from the core

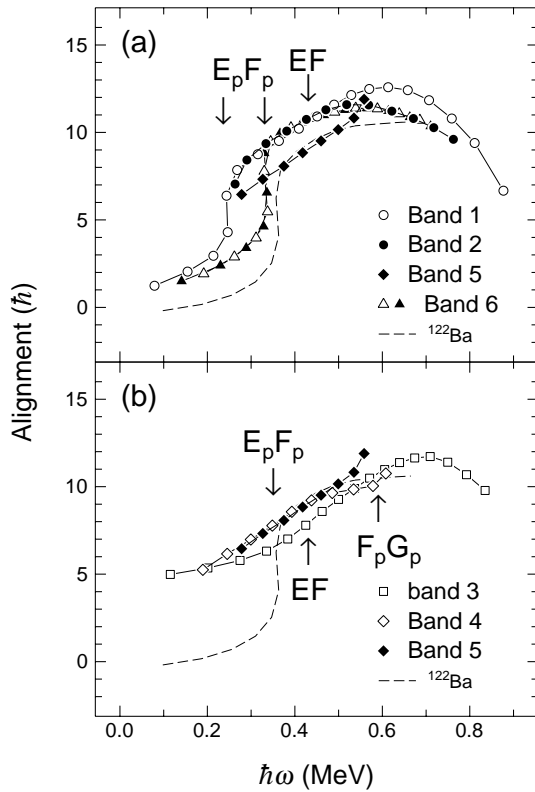


FIG. 4. Aligned angular momentum vs rotational frequency for (a) bands 1, 2, 5, and 6, as well as for (b) bands 3, 4, and 5 in ^{123}La . The ground-state band in ^{122}Ba is included for comparison. Harris parameters of $\mathcal{J}_0=17.0 \hbar^2/\text{MeV}$ and $\mathcal{J}_1=25.8 \hbar^4/\text{MeV}^3$ were used to subtract the angular momentum of the core.

nucleus ^{122}Ba [15,16] is also plotted for comparison. Harris parameters [17] of $\mathcal{J}_0=17.0 \hbar^2/\text{MeV}$ and $\mathcal{J}_1=25.8 \hbar^4/\text{MeV}^3$ were adopted from previous studies [10] to subtract the angular momentum of the collective core. Observed band crossings are labeled in Fig. 4 using an alphabetic labeling scheme [18] in which the most favored $h_{11/2}$ protons and neutrons (with signatures $\alpha=-\frac{1}{2}$ and $+\frac{1}{2}$) are denoted as E_p , F_p and E , F , respectively. The second favored pair of $h_{11/2}$ protons are known as G_p and H_p . Cranked shell model (CSM) [19] calculations were performed using deformation parameters (β_2 , β_4 , and γ) determined by total Routhian surface (TRS) calculations [20] in order to interpret the observed crossings and are presented in Fig. 5. With a predicted ground-state deformation of $\beta_2=0.27$ for ^{123}La , the bands based on the $h_{11/2}[550]1/2$, $d_{5/2}[420]1/2$, $g_{7/2}[422]3/2$, and $g_{9/2}[404]9/2$ orbitals were previously suggested to be near the Fermi surface at $Z=57$ [10]. Band characteristics such as alignment behavior and $B(M1)/B(E2)$ ratios are discussed to associate the observed bands in ^{123}La with the orbitals mentioned above.

1. Band 1

A large alignment gain is observed at a crossing frequency of $\hbar\omega_c \approx 0.26 \text{ MeV}$ for band 1. As seen in Fig. 4(a), the ground-state band in ^{122}Ba displays a similar gain in alignment, but the crossing occurs at a higher frequency of $\hbar\omega_c$

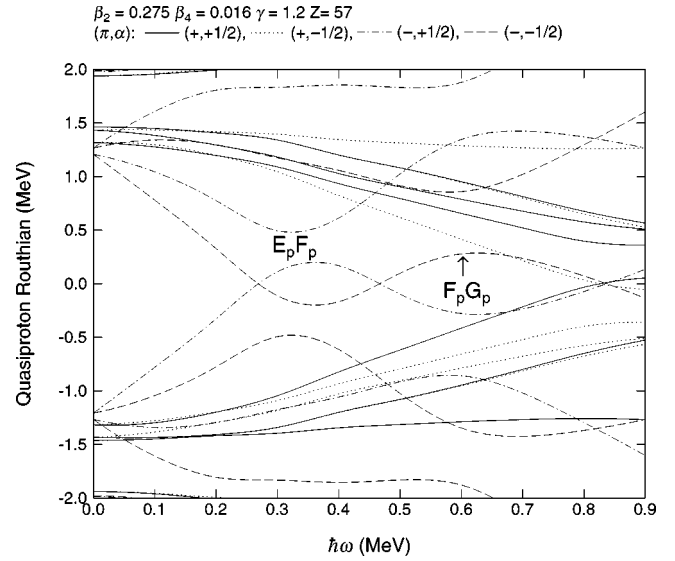


FIG. 5. Quasiproton Routhians calculated within the cranked shell model for ^{123}La . Deformations are listed in the figure and were derived from total Routhian surface calculations.

$\approx 0.36 \text{ MeV}$. Both crossings are interpreted as resulting from the alignment of the lowest $h_{11/2}$ quasiprotons ($E_p F_p$) which are the only orbitals near the Fermi surface that can produce this large increase in angular momentum. Since the $E_p F_p$ crossing is observed in band 1, the $[550]1/2$ configuration is ruled out as this crossing would be Pauli blocked. A strongly coupled sequence is expected to be associated with the $[404]9/2$ configuration; thus, band 1 is likely a mixture of the low- K $d_{5/2}$ and $g_{7/2}$ orbitals. Although band 1 is a mixture of these two even-parity states, one can determine which orbital likely dominates the wave function from the observed favored signature. The favored signature is normally dependent upon the j of the shell as $\alpha_j = (1/2)(-1)^{j-1/2}$; thus, $\alpha_j = +\frac{1}{2}$ for $d_{5/2}$ and $\alpha_j = -\frac{1}{2}$ for $g_{7/2}$. As band 1 has $\alpha = -\frac{1}{2}$ and is the most favored even-parity sequence, it is likely best associated with the $g_{7/2}[422]3/2$ orbital. This conclusion is in good agreement with the proposed bandhead spin and the assignment of Ref. [10].

One may note that the CSM calculations predict the $E_p F_p$ crossing to occur near 0.35 MeV (see Fig. 5). Although this prediction appears to be in good agreement with the crossing frequency in the ground-state sequence in ^{122}Ba , it is higher than the experimental crossing frequency observed in band 1. A similar phenomenon was reported for the lowest $(\pi, \alpha) = (+, -\frac{1}{2})$ configuration in $^{125,127,129}\text{La}$ [7,14,6] and ^{121}Cs [21]. Wyss *et al.* [10] investigated the possibility that the influence of quadrupole pairing could be the cause for the difference in crossing frequencies between this sequence and the ground-state band in ^{122}Ba . By including a quadrupole pairing term in the Hamiltonian, it was found that blocking a down-sloping orbital reduces the pairing field. Indeed, their calculations reproduced the crossing frequency for band 1 by reducing the proton pairing gap Δ_p by 25% as compared to that of the ground-state band in ^{122}Ba . Such effects are amplified in regions where the level density is low, in this case when the proton Fermi surface is near the $Z=50$ shell gap.

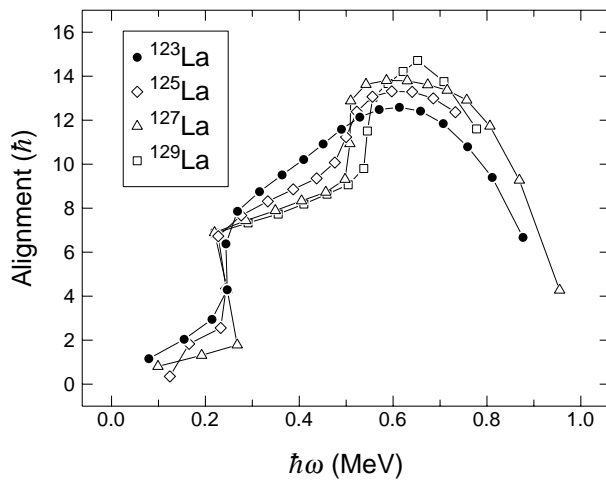


FIG. 6. Alignment of the $[422]3/2$ bands in $^{123,125,127,129}\text{La}$. Harris parameters of $\mathcal{J}_0=17.0 \hbar^2/\text{MeV}$ and $\mathcal{J}_1=25.8 \hbar^4/\text{MeV}^3$ were used for each nucleus.

A gradual gain in alignment is observed in band 1 following the $E_p F_p$ crossing. In order to identify the nature of this rise, the alignments of the $[422]3/2$ bands in $^{123,125,127,129}\text{La}$ are compared in Fig. 6. One may observe that a second crossing, which has been attributed to the rotational alignment of $h_{11/2}$ neutrons (EF crossing), is quite noticeable in the three heavier La isotopes. A trend in the crossing frequency can be established from this plot where the alignment occurs at successively lower frequencies with decreasing neutron number. This is the result of the lowering of the neutron Fermi surface in the $h_{11/2}$ shell such that lower Ω orbitals are occupied. It takes less energy to align the latter orbitals, thus this is an expected trend. Another feature that can be discerned from Fig. 6 is that the interaction strength increased significantly for the EF crossing between ^{125}La and ^{127}La . A systematic study of the EF crossing in Cs nuclei revealed increasing interaction strength as N decreases from 74 to 66 [21]. In fact, ^{121}Cs , the isotone of ^{123}La , displayed the largest interaction strength of all the Cs isotopes. It was suggested that an increase in neutron-proton interactions causes the stronger band mixing [21]. Thus, one may expect a large interaction strength for this crossing in ^{123}La as well, and the alignment gain near 0.44 MeV in band 1 is interpreted as the manifestation of the EF crossing. This frequency is in good agreement with the CSM prediction of $\hbar\omega_c \approx 0.42 \text{ MeV}$ (not shown). The alignment appears to decrease following the EF crossing; however, this is likely to result from improper Harris parameters for the high-frequency, five-quasiparticle region.

2. Band 2

The lowest observed state in band 2 is at 1797.9 keV, suggesting that it is initially a three-quasiparticle structure. Inspection of the alignments for bands 1 and 2, shown in Fig. 4(a), reveals that the two structures have nearly overlapping values between $\hbar\omega=0.25\text{--}0.45 \text{ MeV}$. This indicates that band 2 is observed following the $E_p F_p$ crossing that likely occurred at a low crossing frequency as seen in band 1. Thus,

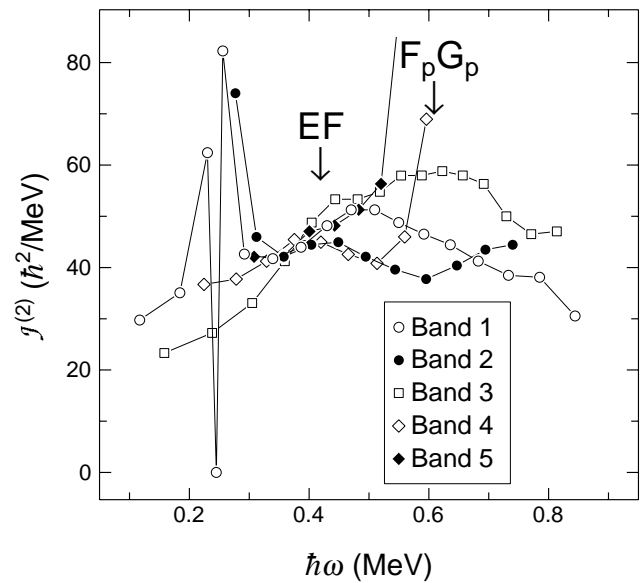


FIG. 7. Dynamic moments of inertia for bands 1–5 in ^{123}La . The EF and $F_p G_p$ crossings are shown in the figure.

it is most plausible that bands 1 and 2 have similar configurations, and the latter is assigned the $\pi(d_{5/2}/g_{7/2}) E_p F_p$ configuration. Since band 2 has the opposite signature of band 1, it is a mixture of the signature partner of band 1 and the favored signature ($\alpha=+1/2$) of the $\pi d_{5/2}$ sequence. The lack of linking transitions between these two sequences suggests that the latter component may be favored. Once again, the gradual gain in alignment near $\hbar\omega=0.4 \text{ MeV}$ is attributed to the EF crossing and no further crossing is observed in band 2 up to $\hbar\omega \approx 0.7 \text{ MeV}$.

3. Band 3

Figure 4(b) displays the aligned angular momentum for band 3. This structure does not experience the low-frequency crossing observed in band 1 or in the ground-state band of ^{122}Ba . Thus, the $E_p F_p$ crossing is blocked, which implies that band 3 is based on the $[550]1/2$ orbital as discussed in Ref. [10]. In addition, the large initial alignment ($\sim 5\hbar$) expected for a high- j , low- K state supports this assignment. An alignment gain is observed to occur over a frequency range of $\hbar\omega_c=0.35\text{--}0.68 \text{ MeV}$ [see Fig. 4(b)]. Inspecting the dynamic moments of inertia ($\mathcal{J}^{(2)}$), which can be a more sensitive indicator of interactions, for bands 1–5 in Fig. 7, one observes a peak near $\hbar\omega_c \approx 0.45 \text{ MeV}$ for band 3. This is similar to the behavior found for bands 1 and 2; therefore, some of the alignment gain is associated with the EF crossing. However, band 3 experiences a second peak in the $\mathcal{J}^{(2)}$ moment near 0.60 MeV that is not observed in bands 1 and 2. This is likely due to the $F_p G_p$ crossing which is predicted to occur at $\hbar\omega_c \approx 0.61 \text{ MeV}$ by the CSM calculations in Fig. 5. This assignment is consistent with the observed $F_p G_p$ crossing at $\hbar\omega_c \approx 0.64 \text{ MeV}$ in the $[550]1/2$ band of ^{125}La [7]. Therefore, the alignment gain observed in Fig. 4(b) for band 3 is the result of both the EF and $F_p G_p$ crossings.

4. Band 4

The energy of the lowest state observed in band 4 (957.1 keV) forbids a three-quasiparticle assignment as this is well below the rotational energy necessary to break a pair of nucleons in ^{123}La . However, the large initial alignment ($\sim 5\hbar$) seen in Fig. 4(b) for this sequence also forbids the $\pi(d_{5/2}/g_{7/2})$ and $\pi g_{9/2}$ configurations, as these orbitals cannot produce such large alignments. Indeed, the only orbital near the Fermi surface that can provide a large initial alignment is the $h_{11/2}$ state. Therefore, there are two possible scenarios for this structure. Band 4 may correspond to the unfavored signature of band 3, in which case the spins would have to be decreased by one unit of \hbar from those shown in Fig. 1. Although this configuration cannot be completely ruled out, such a change in spin would significantly move band 4 away from the yrast line, and this would not be consistent with the observed intensity. Instead, this sequence is proposed to be a quasi- γ -vibrational band based on the $\pi h_{11/2}$ configuration. Structures with similar decay patterns (i.e., with both $I \rightarrow I-2$ and $I \rightarrow I$ linking transitions) and excitation energies have been assigned this configuration in $^{123,125,127}\text{Cs}$ [22–24], $^{124,126}\text{Ba}$ [25,26], ^{125}La [7], and ^{126}Ce [27]. Similar to the analogous structure in ^{125}La , the EF crossing occurs at a slightly lower frequency and has an even larger interaction strength than seen in the pure $\pi h_{11/2}$ sequence (band 3). In addition, at the highest frequencies observed in band 4, there appears to be the beginning of another alignment. This is occurring near the $F_p G_p$ crossing frequency seen in band 3, which is consistent with the proposed assignment.

5. Band 5

A three-quasiparticle assignment is possible for band 5 as the lowest state is observed at 1735.3 keV. The large initial alignment for this structure [see Fig. 4(b)] indicates that at least one $h_{11/2}$ proton is involved in its configuration. It is possible that band 5 has a $\pi(d_{5/2}/g_{7/2})E_p F_p$ configuration. However, its alignment values are consistently $\sim 2\hbar$ lower than those of bands 1 and 2 [see Fig. 4(a)]. One would expect alignment values similar to those of bands 1 and 2 if band 5 has this configuration. Since this is not the case, another scenario has been considered. One may notice that the alignment values of bands 4 and 5 are quite similar below 0.5 MeV [see Fig. 4(b)], which may indicate that the two have related structures. Thus, band 5 could possibly be the unfavored signature of the quasi- γ -vibrational band (band 4). This unfavored signature of the quasi- γ -vibrational band is not often observed in this mass region; however, it was seen to high spin in ^{126}Ba [26]. It was noted in Ref. [26] that the signature splitting was greatly reduced following the $h_{11/2}$ proton alignment, as the latter has the effect of stiffening the nuclear shape. Bands 4 and 5 are found to have some splitting (~ 100 keV), however, this is smaller than the value observed (~ 250 keV) before the proton alignment for γ band in ^{126}Ba . Therefore, the prolate driving $h_{11/2}$ proton, on which the vibration is based in ^{123}La , appears to lessen the splitting between the quasi- γ -vibrational signature partners. While this interpretation is plausible, it is not conclusive and further work is necessary to verify, or disprove, our assignment.

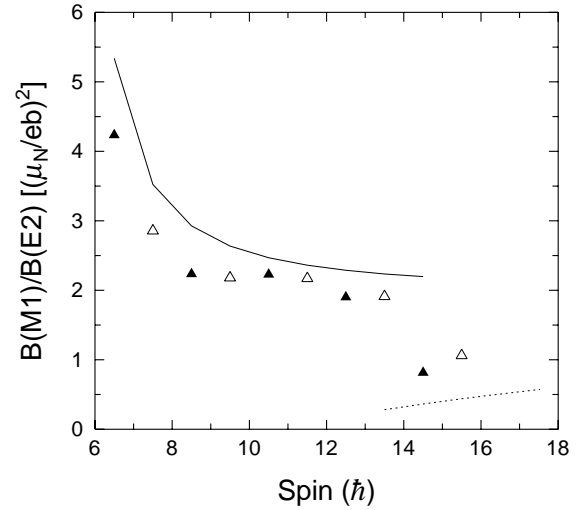


FIG. 8. Experimental (symbols) and theoretical (lines) $B(M1)/B(E2)$ ratios for band 6 in ^{123}La . The parameters used for the calculated values are discussed in the text. The solid and dashed lines represent the $\pi g_{9/2}$ and $\pi g_{9/2} E_p F_p$ configurations, respectively.

6. Band 6

The proton $[404]9/2$ orbital arising from the $g_{9/2}$ shell is the closest high- K state near the ^{123}La Fermi surface at prolate deformation. A strongly coupled structure is expected for this configuration, thus, band 6 appears to be a good candidate for this excitation, as suggested in Ref. [10]. The alignment plot of band 6, shown in Fig. 4(a), displays a crossing at $\hbar\omega_c \approx 0.34$ MeV. The crossing frequency and alignment gain appear to be consistent with those observed in the ground-state band of ^{122}Ba . It was concluded in Ref. [15] that the total alignment gain in the ground-state band of ^{122}Ba resulted from a combination of the $E_p F_p$ and EF crossings. Thus, these same alignments are associated with the increase of $\sim 11\hbar$ observed for band 6 in Fig. 4(a). The reduced $E_p F_p$ crossing frequency is not observed with the $\pi g_{9/2}$ band as blocking this up-sloping orbital (versus as down-sloping orbital, as in band 1), only has a small effect on the pairing field [28].

In order to further confirm this configuration for band 6, the $B(M1)/B(E2)$ ratios were extracted and compared with theoretical predictions. Experimental $B(M1)/B(E2)$ ratios were determined from the observed γ -ray energies and branching ratios according to the standard formula [29]. The results of the $B(M1)/B(E2)$ analysis are displayed in Fig. 8 along with the results of the theoretical calculations. The rotational model form of the $B(E2)$ transition strength [29] and an extended formalism [30] of the geometrical model from Dönau [31] and Frauendorf [32] for the $B(M1)$ strength were used to calculate theoretical $B(M1)/B(E2)$ ratios. An intrinsic quadrupole moment of $Q_0 = 4.58$ e b from the TRS prediction¹ of $\beta_2 = 0.285$ was assumed for the $\pi g_{9/2}$ state. The collective gyromagnetic ratio was taken as $g_R = Z/A$ while $g_K([404]9/2) = 1.27$ and $g_K([550]1/2) = 1.17$ factors were de-

¹The TRS calculations predict a slightly larger deformation for this structure than the other sequences in ^{123}La .

terminated from a Woods-Saxon potential calculation. Initial alignment values for the one quasiparticle and three quasiparticle configurations were obtained from Fig. 4(a). The measured $B(M1)/B(E2)$ ratios show good agreement with the theoretical values for the $[404]9/2$ orbital at a lower spin although a small overestimation is found in the calculated quantities, which may indicate a higher deformation than that predicted by the TRS calculations. A good fit between experimental and calculated ratios is also achieved above $I = \frac{29}{2}$ when assuming a $\pi g_{9/2} E_p F_p$ assignment at higher spins.

B. Nilsson-Strutinsky calculations

A well-deformed nucleus usually increases its angular momentum by collective rotation. However, the collective angular momentum is built from contributions of the different nucleons outside closed shells (the valence nucleons) and is therefore limited. In a specific configuration, the contributions from the valence nucleons may reach their maximal value at some high-spin state. In such a *terminating state* $[4,33]$, all spin vectors are quantized along the rotation axis and the angular momentum is built as the sum of the *aligned spins* from individual nucleons (and nucleon holes) outside a closed shell. On its way to termination, a particular configuration will generally evolve continuously from high collectivity at low spin to a noncollective state at the highest spin. In doing so, the nucleus migrates from a prolate deformation ($\gamma=0^\circ$) through the (ε, γ) plane to an oblate ($\gamma=60^\circ$) shape as angular momentum increases. This shape evolution has been termed as (smooth) band termination. Bands associated with this phenomenon have been identified in $A \sim 110$ nuclei $[4,34,35]$. The corresponding configurations have one or two protons in $h_{11/2}$ orbitals and two proton holes in $g_{9/2}$ orbitals ($2p-2h$ excitations across the $Z=50$ shell gap).

As the proton number increases above $Z=53$, the terminating states involving proton holes will become experimentally inaccessible because they have very high spin and become unfavored energetically. Instead, terminating bands based on configurations with a closed proton core may be observed. These configurations are analogous to those of the terminating bands in Dy/Er nuclei $[36-38]$ in the sense that either the proton or the neutron configuration has a few particles outside a closed core ($Z=50$ and $N=82$) combined with a few neutrons or protons outside a “semiclosed” core of 64 neutrons or protons. Often a few holes in this core are present. Theoretical calculations $[39]$ suggested that the La isotopes would represent good cases to study band termination in configurations with a few holes in the $N=64$ core. In these configurations, the maximum spin value is $I=40-50$. Recent work on heavier La nuclei provided the first experimental evidence that smooth band termination may indeed exist in $^{127,129}\text{La}$ $[5,6]$.

It is a general signature of smooth band termination that a minimum appears in a plot of the excitation energy minus a rigid rotor reference ($E-E_{RLD}$) versus spin. This minimum is a manifestation of the limited available angular momentum that can be generated for the configuration involved. Such evidence appears in Fig. 9 for the lowest $(\pi, \alpha)=(+, -)$ bands in $^{127,129}\text{La}$ $[5,6]$, and, apparently, also for band 1 in ^{123}La .

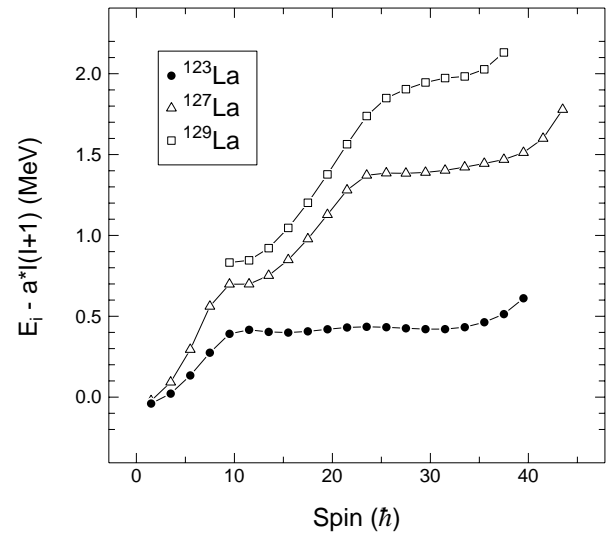


FIG. 9. Excitation energy of states minus a rigid-rotor reference ($E-E_{RLD}$) vs spin for the lowest $(+, -\frac{1}{2})$ sequences in $^{123,127,129}\text{La}$. The A -dependent constant a was determined by scaling $a = 0.007$ MeV for $A=158$ by $A^{-5/3}$ $[4]$ for each nucleus. This leads to a value of $a=0.01063$ MeV for ^{123}La .

One observes for band 1 a constant value (~ 0.4 MeV) over the large spin range of $I \sim 10-33$ in the $E-E_{RLD}$ plot, followed by an increase in energy, similar to that found in the terminating bands of $^{127,129}\text{La}$. Another indication of terminating states is that the dynamic moment of inertia $\mathcal{J}^{(2)}$ decreases continuously as a function of rotational frequency and reaches the minimum value at the terminating point $[4]$. From our experimental data, a decline in $\mathcal{J}^{(2)}$ is observed for band 1 in ^{123}La (see Fig. 7). Thus, at rotational frequencies above ~ 0.65 MeV, the observed $\mathcal{J}^{(2)}$ is considerably below the rigid rotor value $\mathcal{J}_{rig} \approx 45\hbar^2/\text{MeV}$.

In order to investigate whether the observed phenomena are the result of smooth band termination, cranked Nilsson-Strutinsky (CNS) calculations were performed similar to those described in Refs. $[5,6]$. The results are shown together with experimental data for bands 1–3 in Fig. 10. Since pairing is not included in the calculations, the results are realistic only above spin values of approximately 25, but they can provide a general description of the most important configurations also at lower angular momentum. The configurations relative to the $^{100}_{50}\text{Sn}_{50}$ core were defined using the following nomenclature $[4]$:

$$[p_1 p_2, n] \equiv \pi(g_{9/2})^{-p_1}(h_{11/2})^{p_2}(g_{7/2}d_{5/2})^{Z-50+p_1-p_2} \otimes \nu(h_{11/2})^n(g_{7/2}d_{5/2}d_{3/2}s_{1/2})^{(N-50-n)},$$

i.e., p_1 is the number of proton holes in the $g_{9/2}$ orbitals, p_2 is the number of proton $h_{11/2}$ particles, and n is the number of neutrons in the $h_{11/2}$ orbitals. The parity of the configurations is determined by $\pi_{tot}=(-1)^{(p_2+n)}$.

Band 1 in ^{123}La is assigned to the $[422]3/2$ configuration at low spin, suggesting that this structure should have an even number of $h_{11/2}$ protons in the unpaired regime. Comparison of the calculations $[Fig. 10(a)]$ with the experimental values above $I \sim 30$ indicates that the $[2,6]$ configuration de-

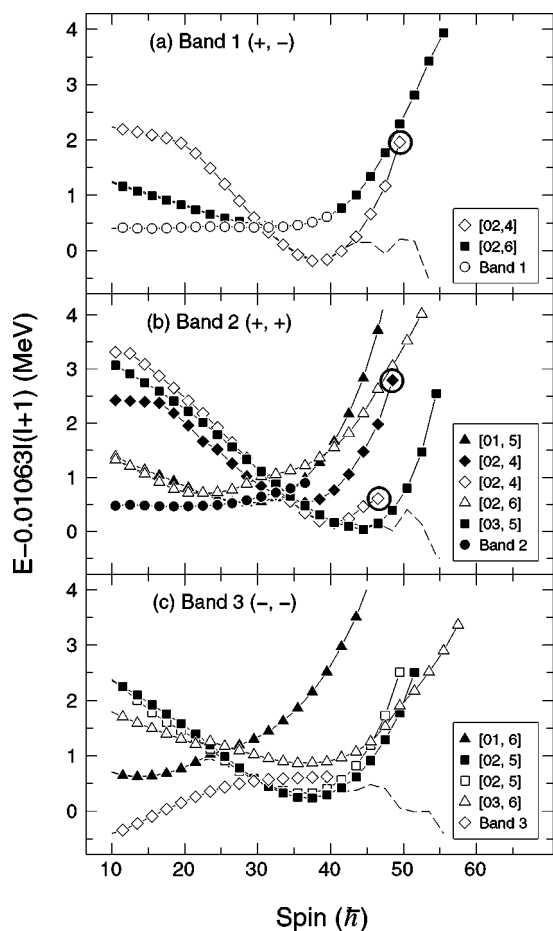


FIG. 10. Comparison of experimental and theoretical $E-E_{RLD}$ energies. Cranked Nilsson-Strutinsky calculations described in the text produced the theoretical curves. Predicted terminating states are marked with a circle encompassing the symbol. The calculated yrast line for the given configuration is displayed as the dashed line in each panel.

scribes band 1 best. The studies of heavier La isotopes [6] reported that the [2,8] configuration was associated with the lower spin states of the [422]3/2 bands and was typically crossed by the [2,6] configuration, which leads to the terminating state. It was found that the spin of this crossing was very close to the spin of the $h_{11/2}$ neutron alignment as well. Following the analogous case for ^{123}La , the [2,4] configuration crosses the [2,6] configuration at $I \approx 30$ and terminates at $I = \frac{99}{2}$ [see Fig. 10(a)]. However, the profile of band 1 does not correspond to that calculated for the [2,4] configuration. In addition, the crossing at $I \approx 30$ does not agree with the experimentally observed band, where it was suggested that the $h_{11/2}$ neutrons align gradually near $I=20$. Since the neutron $h_{11/2}$ alignment in band 1 is occurring over a large range in frequency, it is difficult to observe this effect in the $E-E_{RLD}$ plot. Thus, band 1 appears to remain in the [2,6] configuration, contrary to the smooth band terminating effects seen in the heavier La nuclei. As an uncertainty of ~ 500 keV is assumed for these calculations, the [2,4] configuration may lie higher in energy than suggested in Fig. 10. Another possibility is that the [2,4] band is indeed lower in energy in some spin range, but has not yet been observed.

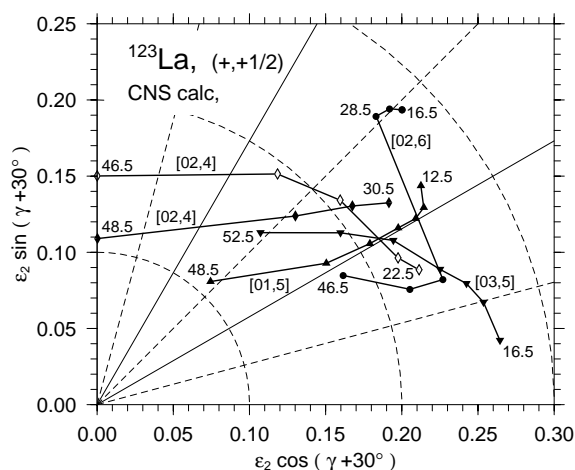


FIG. 11. Calculated shape trajectories for the $(\pi, \alpha)=(+, +)$ configurations of ^{123}La whose $E-E_{RLD}$ curves are drawn in Fig. 10(b). The equilibrium deformations for the different configurations are drawn in angular momentum steps of $6\hbar$.

Band 2 was assigned a $\pi(g_{7/2}/d_{5/2})E_p F_p$ configuration, suggesting that it has a [2,6] configuration at high spin, although it is rather better described as a [1,5] configuration in Fig. 10(b). The irregular energies of the [2,6] $(\pi, \alpha)=(+, +)$ band are caused by a broad energy minimum extending over $|\gamma| \leq 20^\circ$, with the minimum jumping from positive to negative γ values with increasing spin, see Fig. 11. The true minimum would probably be described as a linear combination of these “two minima,” resulting in a smoother energy curve. Once again, the calculated crossing of the [2,6] configuration by the [2,4] sequence is near $I=30$, but the alignment plot in Fig. 4(a) indicates that the $h_{11/2}$ neutrons align gradually near $I=20$. Thus, our experimental results indicate that bands 1 and 2 stay in [2,6] configurations, contrary to those seen in $^{127,129}\text{La}$.

For band 3, shown in Fig. 10(c), the calculations suggest that, in the unpaired regime, this band is associated with the [1,6] configuration at low spins and then with the [3,6] sequence at higher spins. At $I \approx 25$, the [3,6] configuration crosses the [1,6] configuration, which reproduces the $h_{11/2}$ proton alignment qualitatively. Indeed, in Sec. IV A 3 above, this band was assigned as built on an odd $h_{11/2}$ proton at low spin and as containing two additional aligned protons at high spin. With this interpretation, it must have at least three $h_{11/2}$ protons at high spin, i.e., the unpaired and paired calculations give strong mutual support to the respective assignments. A difficulty with the present interpretation is that the unobserved [2,5] configuration is calculated to lie 500–600 keV lower in energy than the [3,6] configuration. A further problem is that the [2,5] $(-, +)$ configuration (not shown) is calculated to be located at an even lower excitation energy than the $\alpha=-1/2$ band shown in Fig. 10. Indeed, considering that this [2,5], $(\pi, \alpha)=(-, +)$ band is the lowest calculated band in the spin range $I=30-40$, it is difficult to explain why no band with this combination of parity and signature has been observed to high spin.

The present calculations indicate that none of the bands in ^{123}La is observed to spin values close to termination. As seen

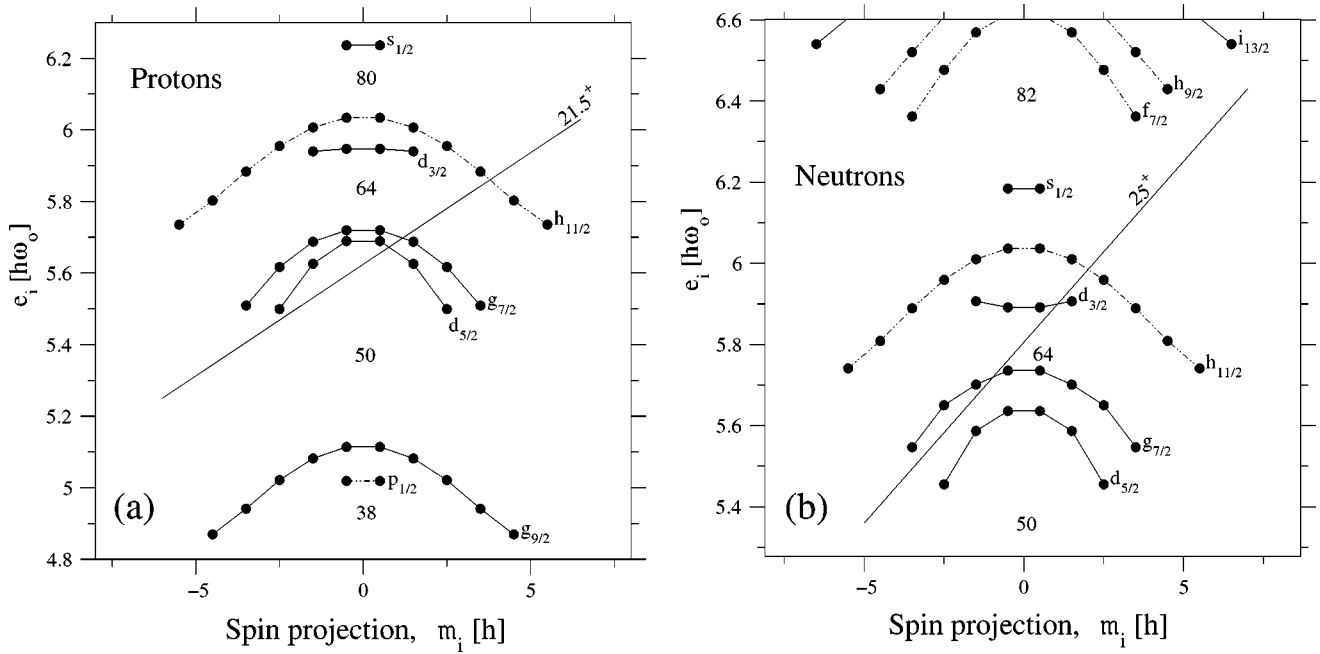


FIG. 12. The single-particle energies e_i at oblate shape drawn vs their spin projection on the symmetry axis, m_i . The deformation, $\varepsilon_2 = 0.125, \varepsilon_4 = 0.025$, is chosen as an average to be approximately correct for those valence space configurations which are calculated to terminate or come close to termination. Straight line sloping Fermi surfaces indicate the occupation of proton and neutron orbitals in the terminating $I=46.5$ state of the [2,4] configuration.

in Fig. 10, only the [2,4] configurations can be followed to termination in the CNS calculations, but these bands are apparently not observed experimentally. Of these [2,4] configurations, the sequence denoted by open diamonds in Fig. 10(b) is perhaps the most interesting as its terminating state (at $I=46.5$) lies only ~ 0.5 MeV above the yrast line. Thus, future experiments may be able to resolve this sequence and follow it to the terminating level herewith providing further tests of the calculations. However, the other [2,4] configurations terminate at levels a few MeV above yrast (see Fig. 10).

The tendencies for different (+,+) configurations to terminate are illustrated in Fig. 11, where the calculated shape trajectories are shown in the (ε, γ) plane. Note that the [2,4] sequence terminating at $I=46.5$ is also shown as open diamonds in Fig. 11, where the deformation values are $\varepsilon=0.15$, $\gamma=60^\circ$ at termination. This noncollective level is built as the maximum-spin state in the $\pi[(h_{11/2})_{10}^2(g_{7/2}d_{5/2})_{11.5}^5]_{21.5} \otimes \nu[(h_{11/2})_{16}^4(g_{7/2}d_{5/2})_{10}^4(d_{3/2})_{1.5}^1]_{25}$ configuration, relative to a $^{114}_{50}\text{Sn}_{64}$ core, where the spin contribution from the different subshells is indicated by the subscripts. This specific state is also depicted in a diagram of the single-particle energies versus spin projection (e_i vs m_i) [4] in Fig. 12. Note that in these terminating states, it is possible to distinguish between orbitals with their main components in the $g_{7/2}/d_{5/2}$ and in the $d_{3/2}$ (or perhaps more properly $d_{3/2}/s_{1/2}$) subshells, respectively. A straight-line Fermi surface representing the configuration above can be drawn for both protons and neutrons in Fig. 12. This configuration is somewhat special in that it involves only one $d_{3/2}$ neutron, which allows the straight line to be drawn in the neutron Fermi surface. In contrast, the [2,4] sequences with higher-lying terminating states both have

neutron configurations involving two $d_{3/2}$ neutrons. The [2,4] sequences with terminating states at $I=48.5$ and 49.5 are represented by $\pi[(h_{11/2})_{10}^2(g_{7/2}d_{5/2})_{10.5,11.5}^5]_{20.5,21.5} \otimes \nu[(h_{11/2})_{16}^4(g_{7/2}d_{5/2})_{10}^4(d_{3/2})_{2.5}^2]_{28}$ relative to a ^{114}Sn core, respectively. A straight-line neutron Fermi surface cannot be drawn for this neutron configuration in Fig. 12(b), and a straight-line proton Fermi surface cannot be drawn for the $I_\pi=20.5$ configuration. Therefore, the terminating states will lie well above the yrast line, as seen in Fig. 10, implying that these terminating states will be difficult to observe experimentally.

The other configurations in Fig. 11 (most notably, the [2,6] configuration associated with band 2) never come close to achieving termination. However, the CNS calculations do attribute the observed minimum in the $E-E_{RLD}$ vs spin plot for band 1 (see Fig. 9) and its decreasing $\mathcal{J}^{(2)}$ (see Fig. 7) to a manifestation of the limited available spin in the configuration. Indeed, it is apparent from Fig. 10 that the limited spin has an important impact on all the calculated configurations, independent of whether the bands terminate or not. In addition, the CNS calculations predict bands of small collectivity in the $I=50-60$ range that terminate on the yrast line. These states have one or several particles in neutron orbitals emerging from the shells above the $N=82$ gap (cf. Fig. 12). The lowest spin, noncollective yrast state of this kind, at $I=101/2^-$, is built from three $h_{11/2}$ protons, four $h_{11/2}$ neutrons, and one $i_{13/2}$ neutron. It terminates at an oblate deformation of $\varepsilon \approx 0.25$.

V. SUMMARY

High-spin states have been investigated in the proton-rich nucleus ^{123}La . Three previously known sequences were ex-

tended to higher spins and three new band structures have been observed. Linking transitions were established for the first time between five of the bands; thus, relative excitation energies are now known. Configurations were proposed for the bands, based upon the observed alignment behavior. The possibility of band 1 displaying characteristics of smooth band termination was explored by comparing the data with cranked Nilsson-Strutinsky calculations. Although a minimum develops in the $E-E_{RLD}$ plot for band 1, the experimental data do not correspond with structures predicted to be near terminating states. It appears that none of the sequences observed in ^{123}La are consistent with predicted smooth band terminating structures. However, the aforementioned minimum is a result of the limited spin available in the configuration. Furthermore, a terminating level at $I=46.5$ with $(\pi, \alpha)=(+, +)$ is predicted to occur relatively close to the

yrast line. Perhaps an experiment with a stronger reaction channel leading to ^{123}La (such as those used in Ref. [10]) and a modern array (such as Gammasphere) will allow for the observation of this low-lying terminating state.

ACKNOWLEDGMENTS

Special thanks to D. C. Radford and H. Q. Jin for their software support. The authors wish to thank the ANL operation staff at Gammasphere. Special thanks also to J. P. Greene for target preparation and use. This work was funded by the U.S. Department of Energy through Contract Nos. DE-FG02-96ER40983 (University of Tennessee), W-31-109-ENG-38 (Argonne National Laboratory), DE-FG05-88ER40406 (Washington University), the National Science Foundation (USNA), the Swedish Research Council, and the Crafoord Foundation (Lund).

-
- [1] E. S. Paul, C. W. Beausang, D. B. Fossan, R. Ma, W. F. Piel, Jr., N. Xu, L. Hildingsson, and G. A. Leander, *Phys. Rev. Lett.* **58**, 984 (1987).
 - [2] K. Starosta, T. Koike, C. J. Chiara, D. B. Fossan, D. R. LaFosse, A. A. Hecht, C. W. Beausang, M. A. Caprio, J. R. Cooper, R. Krücken, J. R. Novak, N. V. Zamfir, K. E. Zyrnyski, D. J. Hartley, D. Balabanski, Jing-ye Zhang, S. Frauendorf, and V. I. Dimitrov, *Phys. Rev. Lett.* **86**, 971 (2001).
 - [3] R. A. Bark, A. M. Baxter, A. P. Byrne, G. D. Dracoulis, T. Kibedi, T. R. McGoram, and S. M. Mullins, *Nucl. Phys.* **A691**, 577 (2001).
 - [4] A. V. Afanasjev, D. B. Fossan, G. J. Lane, and I. Ragnarsson, *Phys. Rep.* **322**, 1 (1999).
 - [5] C. M. Parry, R. Wadsworth, A. N. Wilson, A. J. Boston, P. J. Nolan, E. S. Paul, J. A. Sampson, A. T. Semple, C. Foin, J. Genevey, A. Gizon, J. Gizon, I. Ragnarsson, and B. G. Dong, *Phys. Rev. C* **61**, 021303(R) (2000).
 - [6] R. Wadsworth, E. S. Paul, A. Astier, D. Bazzacco, A. J. Boston, N. Bufo, C. J. Chiara, D. B. Fossan, C. Fox, J. Gizon, D. G. Jenkins, N. S. Kelsall, T. Koike, D. R. LaFosse, S. Lunardi, P. J. Nolan, B. M. Nyakó, C. M. Petrache, H. Scraggs, K. Starosta, J. Timár, A. Walker, A. N. Wilson, L. Zolnai, B. G. Dong, and I. Ragnarsson, *Phys. Rev. C* **62**, 034315 (2000).
 - [7] D. J. Hartley, L. L. Riedinger, H. Q. Jin, W. Reviol, B. H. Smith, A. Galindo-Uribarri, D. G. Sarantites, D. R. LaFosse, J. N. Wilson, and S. M. Mullins, *Phys. Rev. C* **60**, 014308 (1999).
 - [8] R. V. F. Janssens and F. S. Stephens, *Nucl. Phys. News* **6**, 9 (1996).
 - [9] D. G. Sarantites, P. -F. Hua, M. Devlin, L. G. Sobotka, J. Elson, J. T. Hood, D. R. LaFosse, J. E. Sarantites, and M. R. Maier, *Nucl. Instrum. Methods Phys. Res. A* **381**, 418 (1996).
 - [10] R. Wyss, F. Lidén, J. Nyberg, A. Johnson, D. J. G. Love, A. H. Nelson, D. W. Banes, J. Simpson, A. Kirwan, and R. Bengtsson, *Nucl. Phys.* **A503**, 244 (1989).
 - [11] D. C. Radford, *Nucl. Instrum. Methods Phys. Res. A* **361**, 297 (1995).
 - [12] H. Iimura, M. Shibata, S.-I. Ichikawa, T. Sekine, M. Oshima, N. Shinohara, M. Miyachi, A. Osa, H. Yamamoto, and K. Kawade, *J. Phys. Soc. Jpn.* **60**, 3585 (1991).
 - [13] K. E. G. Löbner, in *The Electromagnetic Interaction in Nuclear Spectroscopy*, edited by W. D. Hamilton (North-Holland, Oxford, 1975), p. 141.
 - [14] K. Starosta, Ch. Droste, T. Morek, J. Srebrny, D. B. Fossan, D. R. LaFosse, H. Schnare, I. Thorslund, P. Vaska, M. P. Waring, W. Satula, S. G. Rohozinski, R. Wyss, I. M. Hibbert, R. Wadsworth, K. Hauschild, C. W. Beausang, S. A. Forbes, P. J. Nolan, and E. S. Paul, *Phys. Rev. C* **53**, 137 (1996).
 - [15] R. Wyss, A. Johnson, F. Lidén, J. Nyberg, D. J. G. Love, A. H. Nelson, D. Banes, A. Kirwan, and J. Simpson, in *Proceedings of XXV International Winter Meeting on Nuclear Physics, Bormio, 1987*, edited by I. Iori (University of Milano), p. 542.
 - [16] C. M. Petrache, G. Lo Bianco, D. Bazzacco, Th. Kröll, S. Lunardi, R. Menegazzo, M. Nespolo, P. Pavan, C. Rossi Alvarez, G. de Angelis, E. Farnea, T. Martinez, N. Marginean, D. R. Napoli, and N. Blasi, *Eur. Phys. J. A* **12**, 135 (2001).
 - [17] S. M. Harris, *Phys. Rev.* **138**, B509 (1965).
 - [18] R. Bengtsson, S. Frauendorf, and F.-R. May, *At. Data Nucl. Data Tables* **35**, 15 (1986).
 - [19] R. Bengtsson and S. Frauendorf, *Nucl. Phys.* **A314**, 27 (1979); **A327**, 139 (1979).
 - [20] R. Wyss, J. Nyberg, A. Johnson, R. Bengtsson, and W. Nazarewicz, *Phys. Lett. B* **215**, 211 (1988).
 - [21] F. Lidén, B. Cederwall, P. Ahonen, D. W. Banes, B. Fant, J. Gascon, L. Hildingsson, A. Johnson, S. Juutinen, A. Kirwan, D. J. G. Love, S. Mitarai, J. Mukai, A. H. Nelson, J. Nyberg, J. Simpson, and R. Wyss, *Nucl. Phys.* **A550**, 365 (1992).
 - [22] J. R. Hughes, D. B. Fossan, D. R. LaFosse, Y. Liang, P. Vaska, M. P. Waring, and J.-Y. Zhang, *Phys. Rev. C* **45**, 2177 (1992).
 - [23] J. R. Hughes, D. B. Fossan, D. R. LaFosse, Y. Liang, P. Vaska, and M. P. Waring, *Phys. Rev. C* **44**, 2390 (1991).
 - [24] Y. Liang, R. Ma, E. S. Paul, N. Xu, D. B. Fossan, and R. A. Wyss, *Phys. Rev. C* **42**, 890 (1990).
 - [25] S. Pilotte, S. Flibotte, S. Monaro, N. Nadon, D. Prévost, P. Taras, H. R. Andrews, D. Horn, V. P. Janzen, D. C. Radford, D. Ward, J. K. Johansson, J. C. Waddington, T. E. Drake, A.

- Galindo-Uribarri, and R. Wyss, Nucl. Phys. **A514**, 545 (1990).
- [26] D. Ward, V. P. Janzen, H. R. Andrews, D. C. Radford, G. C. Ball, D. Horn, J. C. Waddington, J. K. Johansson, F. Banville, J. Gascon, S. Monaro, N. Nadon, S. Pilotte, D. Prevost, P. Taras, and R. Wyss, Nucl. Phys. **A529**, 315 (1991).
- [27] A. N. Wilson, R. Wadsworth, J. F. Smith, S. J. Freeman, M. J. Leddy, C. J. Chiara, D. B. Fossan, D. R. LaFosse, K. Starosta, M. Devlin, D. G. Sarantites, J. N. Wilson, M. P. Carpenter, C. N. Davids, R. V. F. Janssens, D. Seweryniak, and R. Wyss, Phys. Rev. C **63**, 054307 (2001).
- [28] M. Diebel, Nucl. Phys. **A419**, 221 (1984).
- [29] A. Bohr and B. R. Mottelson, *Nuclear Structure* (Benjamin, New York, 1975), Vol. 2.
- [30] V. P. Janzen, Z.-M. Liu, M. P. Carpenter, L. H. Courtney, H.-Q. Jin, A. J. Larabee, L. L. Riedinger, J. K. Johansson, D. G. Popescu, J. C. Waddington, S. Monaro, S. Pilotte, and F. Döna, Phys. Rev. C **45**, 613 (1992).
- [31] F. Döna, Nucl. Phys. **A471**, 469 (1987).
- [32] S. Frauendorf, Phys. Lett. **100B**, 219 (1981).
- [33] T. Bengtsson and I. Ragnarsson, Phys. Scr., T **5**, 165 (1983).
- [34] A. V. Afanasjev and I. Ragnarsson, Nucl. Phys. **A591**, 387 (1995).
- [35] R. Wadsworth, R. M. Clark, J. A. Cameron, D. B. Fossan, I. M. Hibbert, V. P. Janzen, R. Krücken, G. J. Lane, I. Y. Lee, A. O. Macchiavelli, C. M. Parry, J. M. Sears, J. F. Smith, A. V. Afanasjev, and I. Ragnarsson, Phys. Rev. Lett. **80**, 1174 (1998).
- [36] I. Ragnarsson, Lawrence Berkeley Laboratory Report No. LBL-22379, 1986 (unpublished).
- [37] F. G. Kondev, M. A. Riley, R. V. F. Janssens, J. Simpson, A. V. Afanasjev, I. Ragnarsson, I. Ahmad, D. J. Blumenthal, T. B. Brown, M. P. Carpenter, P. Fallon, S. M. Fischer, G. Hackman, D. J. Hartley, C. A. Kalfas, T. L. Khoo, T. Lauritsen, W. C. Ma, D. Nisius, J. F. Sharpey-Schafer, and P. G. Varmette, Phys. Lett. B **437**, 35 (1998).
- [38] W. C. Ma, R. V. F. Janssens, T. L. Khoo, I. Ragnarsson, M. A. Riley, M. P. Carpenter, J. R. Terry, J. P. Zhang, I. Ahmad, P. Bhattacharyya, P. J. Daly, S. M. Fischer, J. H. Hamilton, T. Lauritsen, D. T. Nisius, A. V. Ramayya, R. K. Vadapalli, P. G. Varmette, J. W. Watson, C. T. Zhang, and S. J. Zhu, Phys. Rev. C **65**, 034312 (2002).
- [39] A. V. Afanasjev and I. Ragnarsson, Nucl. Phys. **A608**, 176 (1996).